# Recovering Higher Order Modes in the Ringdown of Binary Black Hole Coalescences

**LIGO Caltech SURF Interim Report 2**
**LIGO Document**

Rachel Mechum*
*University of Florida*

Mentors: Richard Udall† and Alan Weinstein‡
*California Institute of Technology*
*LIGO Laboratory, Caltech*
(Dated: August 1st, 2022)

Disturbances in the curvature of spacetime from the coalescence of binary black holes can be probed by the gravitational waves of radiation emitted by these sources and recorded by Advanced LIGO and Virgo. The merger of such objects allows us to test Einstein's theory of general relativity in the regime of strong and highly dynamical gravity - specifically, the newly formed black hole rings down in a series of quasinormal modes, whose frequencies and damping rates are fully predicted by general relativity. We focus on the ringdown of the remnant black hole, implementing ringdown analysis in the time domain. We demonstrate the ability to fit and recover higher order modes of the ringdown within the simulated IMR signal. Possible deviations of the frequencies and damping times of the ringdown may point to new physics beyond general relativity, such as quantum gravity that we are not yet familiar with.

**Keywords:** gravitational waves, general relativity, LIGO, quasinormal modes, compact binary mergers

## I. MOTIVATION

Gravitational wave (GW) signals from compact binary coalescences (CBC) provide crucial information to understand what remains of the remnant black hole (BH) and allow us to test general relativity (GR) in the regime of strong and highly dynamical gravity.

Binary neutron stars (BNS), black hole-neutron star (BHNS), and binary black holes (BBH) are the three main classes of detectable CBCs from our current ground-based detectors. Future detectors such as LISA will allow us to study more types of CBCs. More specifically, we will look at BBH merger events. The data from BBH mergers come from real events, but are simulated to better understand our current models and refine our analysis techniques. During a BBH coalescence, there are 3 stages: the inspiral, merger, and ringdown (IMR). The remnant of merged BHs is a single perturbed BH with a GW waveform characterized as a set of complex frequencies and damping times known as quasinormal modes (QNMs), which are unambiguously predicted by GR. The gravitational radiation from this remnant is called the ringdown phase [1].

BH ringdown is an effective probe of GR in the strong field, notably the "no-hair theorem" (NHT). Detections of deviations from GR in the form of violations of NHT can point to physcis beyong GR. We model the ringdown to be a linear superposition of damped sinusoids,

$$\sum_{lmn} A_{lmn} e^{-t/\tau_{lmn}} sin(2\pi f_{lmn} t), \tag{1}$$

where $l$ and $m$ index the angular modes, $n$ is the overtone, $A$ is the amplitude of the waveform, $\tau$ is the damping time, and $f$ is the frequency (see FIG. 1). Compactly, the ringdown is a set of complex frequencies, $\omega$,

$$\omega = 2\pi f + i/\tau, \tag{2}$$

determined by the nature of the remnant black hole [2].

The dominant quasinormal mode in GR is recognized as (220), where $l = 2$, $m = 2$, and $n = 0$. This mode displays the highest frequency and is the least damped, which we label as the fundamental (22) mode. Higher order modes (HOMs) of QNMs are the modes with smaller amplitudes than the dominant (22) mode: (330), ... , (440).

Higher order modes (HOMs) that have a radial mode $n > 0$ are referred to as overtones. Overtones are the QNMs with faster damping times than $n = 0$ [3]. In previous data analysis, the inclusion of overtones was omitted which led to loss of signal content. That is to say, the inclusion of overtones is important to extract the parameters of the signal more accurately [4] and further the field of black hole spectroscopy.

The GW ringdown frequencies and damping times reveal the final mass and spin of the merged BH. The frequencies for a Kerr black hole do not depend upon its dynamical past, but the amplitudes of the ringdown do. This leads to the discussion of the NHT. The NHT states that mass and spin are the only two properties of Kerr BHs in GR. Therefore, they uniquely determine each $f_{lmn}$ and $\tau_{lmn}$. We can test the NHT with the data

* rachel.mechum@ufl.edu
† rudall@caltech.edu
‡ ajw@caltech.edu

collected during previous and future runs of GW detectors [3].

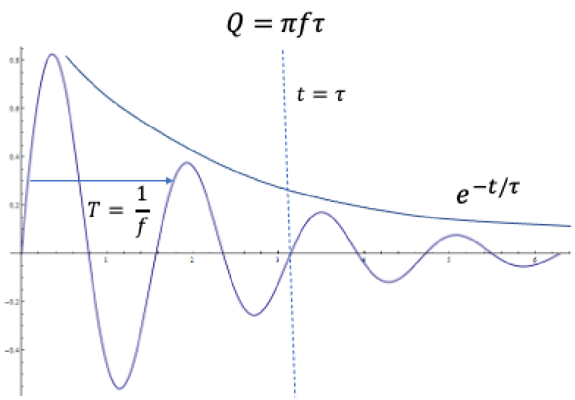


FIG. 1. Example of a singular damped sinusoidal QNM. $T$ is the period, $Q$ is the quality factor, and $e^{-t/\tau}$ is the exponential decay. By setting $t = \tau$, we can see the quality factor will be $\sim 2$. When adding multiple QNMs, the equation will result in a linear superposition of damped sinusoidal oscillations, as seen in Eqn. 1.

## II. APPROACH AND METHODS

Recovering higher order QNMs is a powerful way to test Einstein's theory of GR. This proves to be more difficult once passing the dominant angular mode, ($l = m = 2$). We will use real GW signals from the third LIGO-Virgo observing run (O3), as well as simulated data. The simulated data will be analyzed in the time domain.

The framework for this research is based on work done by Maximiliano Isi and Will Farr, who analyzed ringdowns not in the frequency domain, but in the time domain. However, this approach demands truncating the GW signal at a specific time, which is difficult to handle with the usual LIGO-Virgo analysis techniques. Instead, it calls for special treatment in the time domain, or an equivalent nontrivial procedure in the frequency domain [3, 5–8]. We chose to work with the former and use the *RINGDOWN* software package [5].

Using the *RINGDOWN* software package, we are able to produce simulated ringdowns that are consistent with GR. The simulated ringdown is a 'ringup-ringdown' where the ringdown is symmetrical to the ringup. This does not correspond to real astrophysical events that have been detected.

Making use of the IMRPhenomXP and IMRPhenomXPHM approximants [9], we also simulate a realistic waveform that takes arguments of mass and spin of the two component BHs in the binary. By truncating this signal to show only what happens immediately after merger, we can use this simulated waveform for our various ringdown analyses.

Using this time domain approach to analyze the ringdown waveform, it is necessary to be able to recover the higher order modes from a signal. We begin by using a simulated signal with IMRPhenomXP [9] approximant. From this, we can use a curve fitting method to identify QNMs. The reason for the curve fit approach is to computationally identify different modes rather than identification of various modes by eye. We implement curve fit to show that the signal does truly contain the expected modes and that we are capable of recovery (in the IMRPhenomXP case we only recover the 22 mode since that is the only mode XP includes).

Once establishing that the 22 mode can be recovered along with some of its overtones, we advance to using the IMRPhenomXPHM [9] approximant which includes the addition of higher modes (21, 22, 32, 33, 44). This is our primary goal, to recover HOMs of a simulated waveform to further our confidence when applying this method to real GW data.

## III. RESULTS

When observing the behavior of higher order QNMs we note that with increasing modes comes higher frequencies, lower amplitudes, and shorter damping times. By varying the mass and spin parameters (which result in specific frequencies and damping times of the oscillation), we can note the changes of the waveform. Keeping this in mind, we then have the option to vary other parameters (such as duration of the signal and location) to create a variety of waveforms. This allows us to have a sense of how the waveform should look with different parameters. We begin by simulating a noiseless, time-domain waveform to see how different angular modes and overtones behave.

For these simulated post-merger events, we are able to specify the angular modes, $l$ and $m$, as well as the overtone, $n$. In return, we have access to the frequecies and damping times of different modes and overtones [10]. The primary noiseless waveforms are simulated to analyze the behavior of the ringdown oscillations alone.

### A. Complex Frequencies and Damping Times

As previously stated, all QNMs have their own distinct frequencies and damping times that are derived directly from the mass and spin of the remnant BH. With these frequencies and damping times, we can plot them against respective values of $\chi$ ranging from 0-1 (see FIG. 7-9).

Analyzing the plots, we can see that as by increasing multipoles, their frequency and Q factor is climbing. We can also note that in each leftmost plot, the frequencies of each overtone are spread at $\chi = 0$. The frequencies and damping times diverge towards infinity at $\chi = 1$, but never reach due to the expectation spins of astrophysical BHs ($\chi < 1$).

### B. Dominant Mode and Overtones

When analyzing the fundamental (220) mode, we understand why this is labeled the dominant mode. This mode can be more easily recovered due to how 'loud' it is compared to subdominant modes. Berti et al. [11] showed that the ringdown analysis with only ($l = 2, m = 2, n = 0$) mode can lose 10% of potential LIGO events [1]. Since this fundamental mode behaves just as we expect (by having the highest frequency in the (22) mode and showing to be the least damped), this makes it the best recovery target.

When adding overtones, the frequencies and damping times of the wave decreases. Recovering ringdowns with higher overtones is where the task becomes more difficult. For us to efficiently be able to recover the (22) mode and higher overtones, we would need a louder event or a more sensitive detector.

### C. Subdominant Modes and Overtones

Simulating the subdominant modes along with their overtones is imperative to understand how to deconstruct real waveforms. When we begin recovering these HOMs in true ringdown data, we will know what to search for and soon be confident in what and where the best events are to spot them.

Beginning with the first subdominant angular mode ($l = 3, m = 3, n = 0$), we note an increase in frequency from the dominant fundamental mode ($l = 2, m = 2, n = 0$). The subdominant mode of ($l = m = 3$) is consistent in the decrease in frequency with increasing overtones. We see the same information when simulating the ($l = m = 4$) fundamental mode along with various overtones.

### D. Ringup-Ringdown

By simulating a ringup-ringdown waveform for mutiple HOMs we are able to note that higher modes have higher frequencies and amplitudes. The overtones of these modes reveal lower amplitudes and a small decrease in frequency (see FIG. 2). These plots are a base reference for when simulating real signals, so we know what is expected from the simulated data containing higher modes.

### E. IMRPhenomXP

Moving into IMRPhenomXP, we know that this approximant includes only the 22 angular mode. By adopting a fitting method that specifically fits for the 22 mode, we are able to confidently fit the 22 mode and its respective overtones. Curve fit is looking to fit amplitude and phase to the truncated IMR waveform. When using IMRPhenomXP, since it only possesses the 22 mode we are

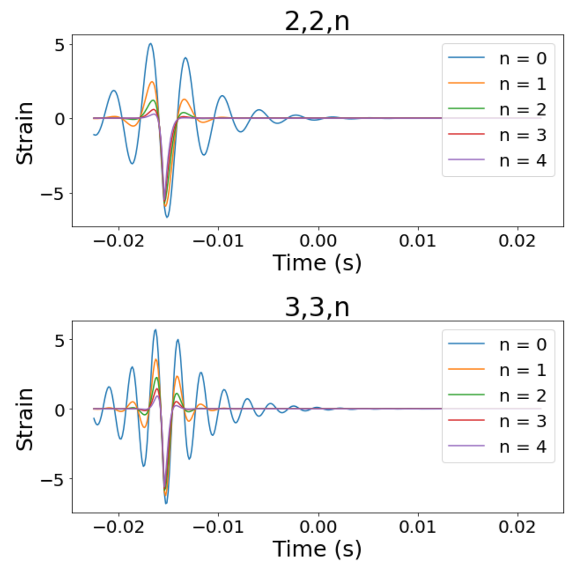


FIG. 2. Increase of amplitude and frequency in HOMs. The oscillation period increases when transitioning from angular mode 22 to 33. The overtones here are also showing the decrease in amplitude and frequency.

able to fully recover the dominant mode along with the first and second overtones. Seemingly strict bounds are placed to allow curve fit to fit more efficiently, as shown in FIG. 3 and FIG 4.

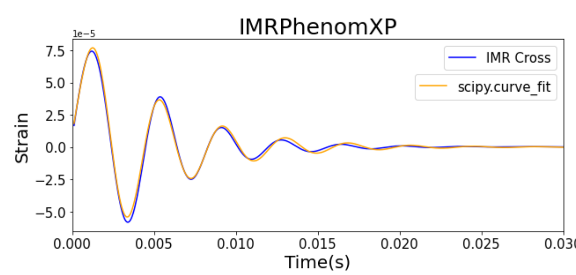


FIG. 3. Curve fitting to the IMRPhenomXP truncated waveform. The fit adapts to the phase and amplitude of the signal.

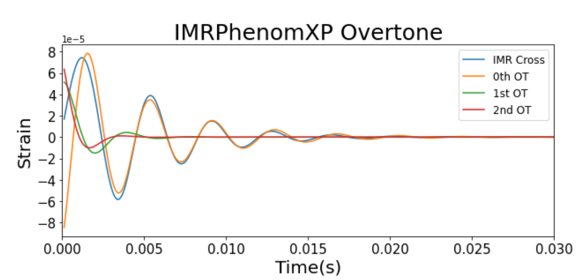


FIG. 4. Plotting the return values of curve fit to the overtones of IMRPhenomXP truncated waveform. This is expected, 220 dominates while the overtones are sub-dominant.

### F. IMRPhenomXPHM

IMRPhenomXPHM has proven to be the most difficult for curve fit to adjust to. There are five modes that all include overtones (summing to be thirty parameters in addition to final mass and spin) that curve fit is challenged with. With the strictest bounds, curve fit still does its best work at the beginning time window of the signal and tends to give a poor fit at later times. I hope to soon improve this method by comparing the residuals of each fit and returning the best possible fits.

When curve fitting IMRPhenomXPHM, the input parameters ultimately determine how well curve fit can recover the full waveform and its modes. The best fit used initial parameters of equal mass and equal spins in the x,y,and z-directions at an inclination of zero (see FIG. 5). The next best curve fit was handled well with parameters of equal mass and negative equal spin in only the z-direction with an inclination of $\pi/2$ as shown in FIG. 6.

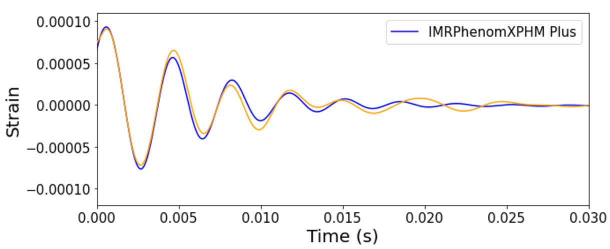


FIG. 5. Curve fit of IMRPhenomXPHM truncated waveform. Parameters of $M_1 = 40, M_2 = 40, \chi_1 = (0.5, 0.5, 0.5), \chi_2 = (0.5, 0.5, 0.5)$ The orange line represents the fit, fitting more accurately from time 0 to 0.011 and later skews off.

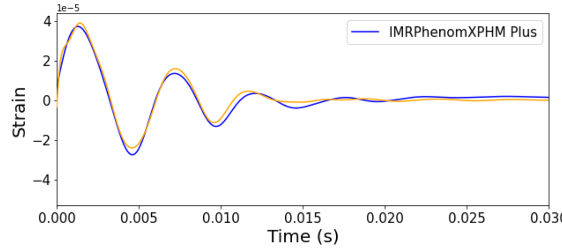


FIG. 6. Curve fit of IMRPhenomXPHM truncated waveform. Parameters of $M_1 = 40, M_2 = 40, \chi_1 = (0, 0, -0.5), \chi_2 = (0, 0, -0.5)$ Orange line representing the fit, again fitting more accurately in the beginning and later dies down.

### G. Next Steps

The next step in this process is attempting to keep residual values to compare what fits are the most accurate. From here, we can determine whether other methods within curve fit should be resourced or if the residual value is low enough that we can accept the fit.

Beyond simulating the fundamental dominant and fundamental subdominant modes along with their respective overtones to explore the raw ringdown waveform, we don't want to just examine the noiseless scenario.

After analyzing and fitting the most basic waveform, we plan to then add Gaussian distributed noise to the simulated ringdown. By adding noise, it will then be possible to explore the recovery of HOMs and their overtones in a more realistic scenario.

## ACKNOWLEDGMENTS

I wish to acknowledge the tremendous support of my mentors, Richard Udall and Alan Weinstein, for offering suggestions and encouragement to help further my research. I also gratefully recognize the support from the National Science Foundation Research Experience for Undergraduates (NSF REU) program, the California Institute of Technology, and the LIGO Laboratory Summer Undergraduate Research Fellowship.

[1] N. Sago, S. Isoyama, and H. Nakano, Fundamental tone and overtones of quasinormal modes in ringdown gravitational waves: A detailed study in black hole perturbation, Universe **7**, 357 (2021).

[2] R. Brito, A. Buonanno, and V. Raymond, Black-hole spectroscopy by making full use of gravitational-wave modeling, Physical Review D **98**, 10.1103/physrevd.98.084038 (2018).

[3] M. Isi, M. Giesler, W. M. Farr, M. A. Scheel, and S. A. Teukolsky, Testing the no-hair theorem with GW150914, Physical Review Letters **123**, 10.1103/physrevlett.123.111102 (2019).

[4] X. Forteza, S. Bhagwat, P. Pani, and V. Ferrari, Spectroscopy of binary black hole ringdown using overtones and angular modes, Physical Review D **102** (2020).

[5] M. Isi and W. M. Farr, Analyzing black-hole ringdowns (2021).

[6] J. Veitch, V. Raymond, B. Farr, W. Farr, P. Graff, S. Vitale, B. Aylott, K. Blackburn, N. Christensen, M. Coughlin, W. D. Pozzo, F. Feroz, J. Gair, C.-J. Haster, V. Kalogera, T. Littenberg, I. Mandel, R. O'Shaughnessy, M. Pitkin, C. Rodriguez, C. Röver,

T. Sidery, R. Smith, M. V. D. Sluys, A. Vecchio, W. Vousden, and L. Wade, Parameter estimation for compact binaries with ground-based gravitational-wave observations using the LALInference software library, Physical Review D **91**, 10.1103/physrevd.91.042003 (2015).

[7] G. Carullo, W. D. Pozzo, and J. Veitch, Observational black hole spectroscopy: A time-domain multimode analysis of GW150914, Physical Review D **99**, 10.1103/physrevd.99.123029 (2019).

[8] C. D. Capano, M. Cabero, J. Westerweck, J. Abedi, S. Kastha, A. H. Nitz, A. B. Nielsen, and B. Krishnan, Observation of a multimode quasi-normal spectrum from a perturbed black hole (2021).

[9] G. Pratten, C. Garcí a-Quirós, M. Colleoni, A. Ramos-Buades, H. Estellés, M. Mateu-Lucena, R. Jaume, M. Haney, D. Keitel, J. E. Thompson, and S. Husa, Computationally efficient models for the dominant and subdominant harmonic modes of precessing binary black holes, Physical Review D **103**, 10.1103/physrevd.103.104056 (2021).

[10] L. C. Stein, Qnm.

[11] E. Berti, J. Cardoso, V. Cardoso, and M. Cavaglià, Matched filtering and parameter estimation of ringdown waveforms, Phys. Rev. D **76**, 104044 (2007).

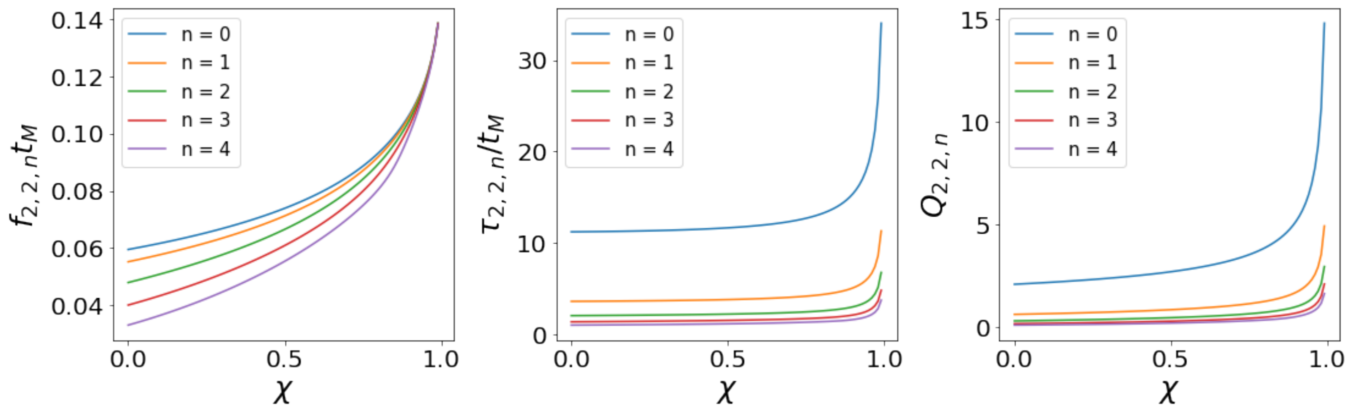


FIG. 7. Frequency $f_{22n}$ (left), damping time $\tau_{22n}$ (center) and quality factor $Q_{22n} = \pi f_{22n}\tau_{22n}$ (right) for changing $l = m = 2$ tones, as a function of dimensionless BH spin $\chi$. Times are measured in units of $t_M \equiv GM/c^3$ for BH mass $M$.

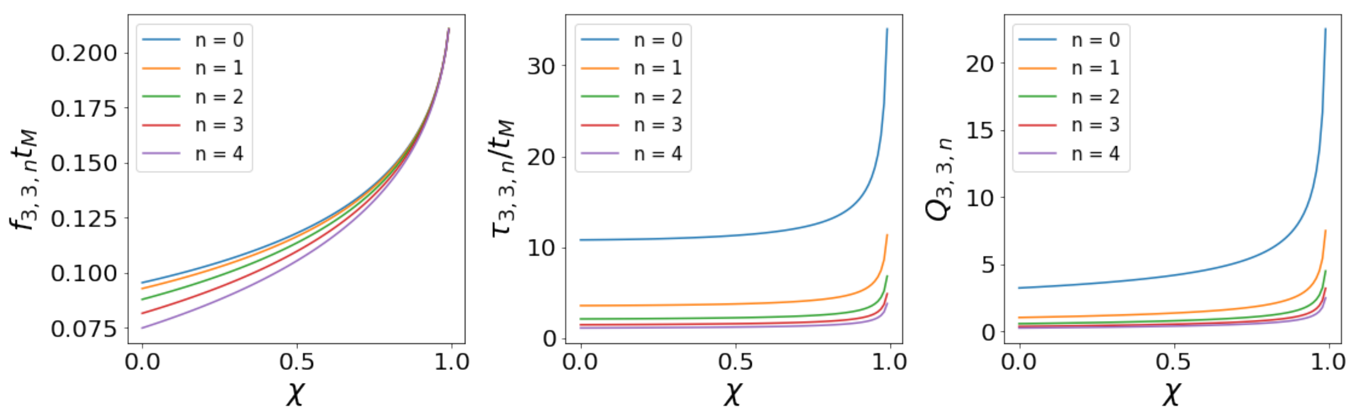


FIG. 8. Frequency $f_{33n}$ (left), damping time $\tau_{33n}$ (center) and quality factor $Q_{33n} = \pi f_{33n}\tau_{33n}$ (right) for changing $l = m = 3$ tones, as a function of dimensionless BH spin $\chi$.

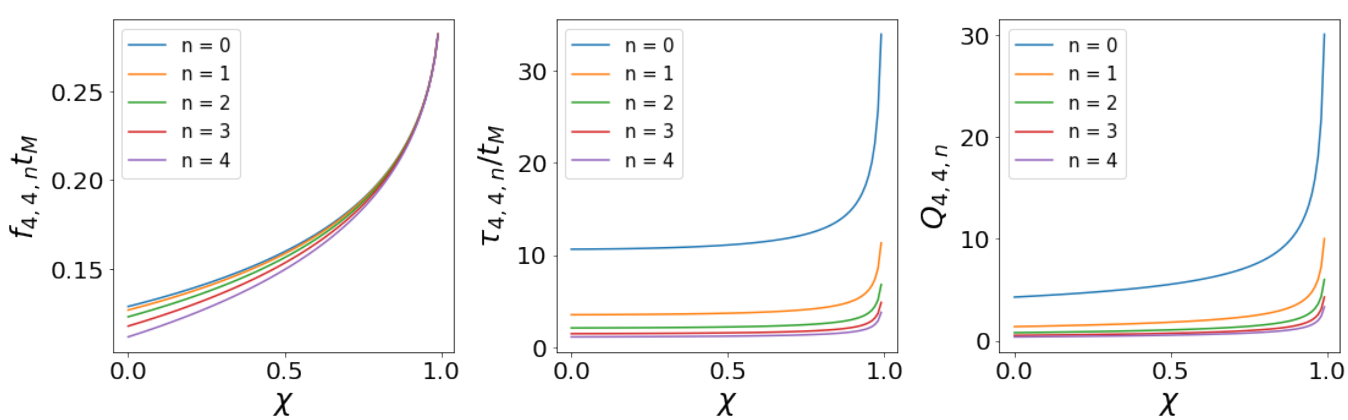


FIG. 9. Frequency $f_{44n}$ (left), damping time $\tau_{44n}$ (center) and quality factor $Q_{44n} = \pi f_{44n}\tau_{44n}$ (right) for changing $l = m = 4$ tones, as a function of dimensionless BH spin $\chi$.